# RFID AND VIRTUAL REALITY TEST SETUP FOR VISUALLY IMPAIRED ASSISTIVE TECHNOLOGY

Ingmar BEŠIĆ, Zikrija AVDAGIĆ, Kerim HODŽIĆ
Department of Computer Science and Informatics, Faculty of Electrical Engineering,
University of Sarajevo, 71000 Sarajevo, Bosnia and Herzegovina, tel. +387 33 250 700,
E-mail: ingmar.besic@etf.unsa.ba, zikrija.avdagic@etf.unsa.ba, kerim.hodzic@etf.unsa.ba

**ABSTRACT**

*Visual impairments often pose serious restrictions on a visually impaired person and there is a considerable number of persons, especially among aging population, which depend on assistive technology to sustain their quality of life. Development and testing of assistive technology for visually impaired requires gathering information and conducting studies on both healthy and visually impaired individuals in a controlled environment. We propose test setup for visually impaired persons by creating RFID based assistive environment – Visual Impairment Friendly RFID Room. The test setup can be used to evaluate RFID object localization and its use by visually impaired persons. To certain extent every impairment has individual characteristics as different individuals may better respond to different subsets of visual information. We use virtual reality prototype to both simulate visual impairment and map full visual information to the subset that visually impaired person can perceive. Time-domain color mapping real-time image processing is used to evaluate the virtual reality prototype targeting color vision deficiency.*

***Keywords:*** *Visual Impairment, Assistive Technology, RFID, Virtual Reality, Image Processing, Color Vision Deficiency*

## 1. INTRODUCTION

Major eye diseases resulting in a vision loss and vision disorders are age-related macular degeneration (AMD), glaucoma, diabetic retinopathy, cataract and refractive error. These pose severe economic burden that might become even higher in the future due to the aging population in developed countries [1]. U.S. statistics show that cataract is by far the most frequent eye disease, followed by diabetic retinopathy, glaucoma and AMD, as can be seen in Fig. 1. Statistics from African countries, like Botswana, have very similar distribution of eye diseases to the U.S having cataract as the most dominant eye condition, as can be seen in Fig. 2. Thus, it seems that eye diseases are not closely related to any specific socio-economic factor [2]. In Europe AMD along with diabetic eye disease (DED) is the main cause of blindness and severe visual loss [3]. Percentage of affected people varies from country to country and late AMD seems to be the most prevalent in Italy and France, as can be seen in Fig. 3. The number of patients affected by AMD in the EU is expected to rise by almost 25% till 2050 [3]. There is also a strong global evidence that significant growth in the number of elderly people experiencing sight loss is likely, despite to significant efforts to prevent blindness [4].

Visually impaired person encounters a range of problems related to her or his everyday tasks. Navigating in indoors environment can be challenging even if the person is familiar with the environment. Even very subtle changes in the environment like half open doors or half open drawer, that are usually not recognized as potentially hazardous by a person with intact vision, can result in injuries or discomfort because visually impaired person cannot easily detect such changes and familiarity with the environment can be deceptive as it tends to project false sense of security. Visually impaired person relies on its cognitive map to navigate, but this map is a snapshot and might not be accurate representation of the current state of the environment. Aids like a white cane are usually used to

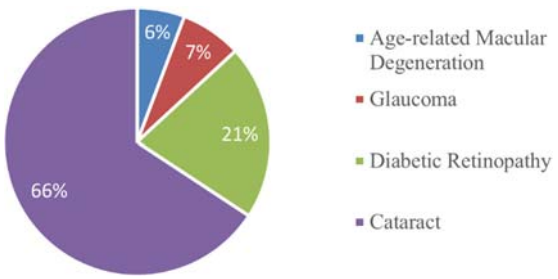


**Fig. 1** Major eye disease statistics, North America (U.S.)

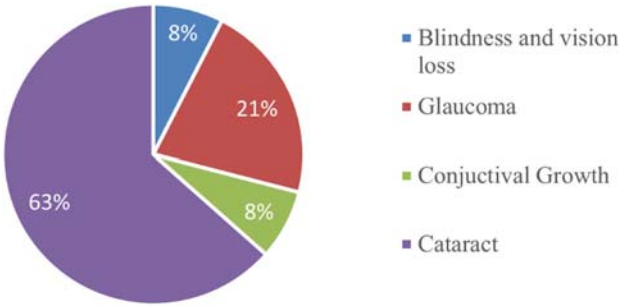


**Fig. 2** Major eye disease statistics, Africa (Botswana)

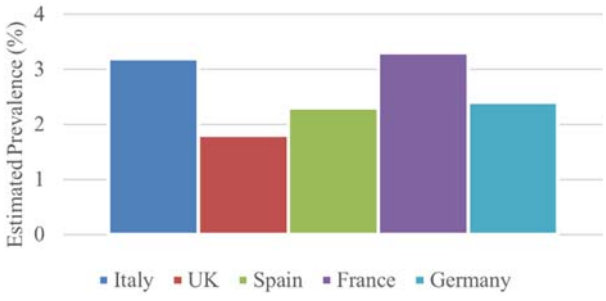


**Fig. 3** Late age-related macular degeneration prevalence in Europe

refresh and update the cognitive map, but such aids have blind spots and cannot detect every change in the environment nor detect every danger in time. Both visually impaired and elderly people experience problems related to locating objects of interest. It can be challenging to cognitively track object location over the period of time and if object is not in plain sight it can be frustrating experience to locate it. In this paper we use RFID technology to create indoors test setup – Visual Impairment Friendly RFID Room. It can be used to evaluate RFID object localization and its use by visually impaired persons [5].

Virtual reality (VR) can stream custom and separate images to both eyes in real-time and thus enables a new class of assistive technology for visually impaired that can deliver visual information in a highly customized manner by targeting only healthy or less damaged part of the retina. If assistive technology is supposed to stream real-time visual information from subject's field of view (FoV) then augmented reality is needed. Virtual reality can be transformed into augmented reality by using optical see-through device or video see-through device [5]. Optical see-through device has the advantage of displaying the reality through a clear optics and thus rendering virtual contents only. However it might introduce mismatches while synchronizing rendered virtual contents with the reality. Video see-through device renders both virtual contents and reality at the same time, possibly resulting in a higher latency but with no synchronization mismatches. In our test setup we propose video see-through assistive technology prototype to avoid synchronization mismatches. The prototype is based on a commercial virtual reality headset and stereo camera [5].

## 2. VISUAL IMPAIRMENT SETUP REQUIREMENTS

In order to create suitable test environment that enables reliable assistive technology development and testing, it is important to understand the effects of various visual impairments. It is also important to compare the benefits of existing treatments to the use of assistive technology and specifically to estimate if VR based assistive technology would be a reasonable choice [5].

Age-related macular degeneration causes central vison loss as can be seen in Fig. 4 top-right. There is no cure for AMD, but some treatments may delay its progression or even improve vision [6]. Visually impaired person suffering from AMD would benefit from the use of assistive technology. VR headset based assistive technology could be used to manipulate field of view (FoV) by transferring some visual information from the damaged central FoV to the peripheral FoV. The result would be limited because visual information would be lost while mapping full FoV to a smaller area. More importantly, visual information would be lost because peripheral vision cannot process visual information at the same level of details as the central vision [5].

Glaucoma initially causes peripheral vision loss, as can be seen in Fig. 4 middle-left. If not treated it eventually results in blindness. Glaucoma can be treated with medicated eye drops, micro-surgery and laser treatments [6]. Unfortunately, glaucoma has no early warning signs and is often diagnosed once the optical nerve has been damaged and the lost vision cannot be restored. Visually impaired person with glaucoma induced damage would benefit from the use of assistive technology. VR headset based assistive technology could be used to manipulate field of view (FoV) by transferring some visual information from the peripheral FoV to the central FoV. The result would be somewhat limited because information loss would occur [5].

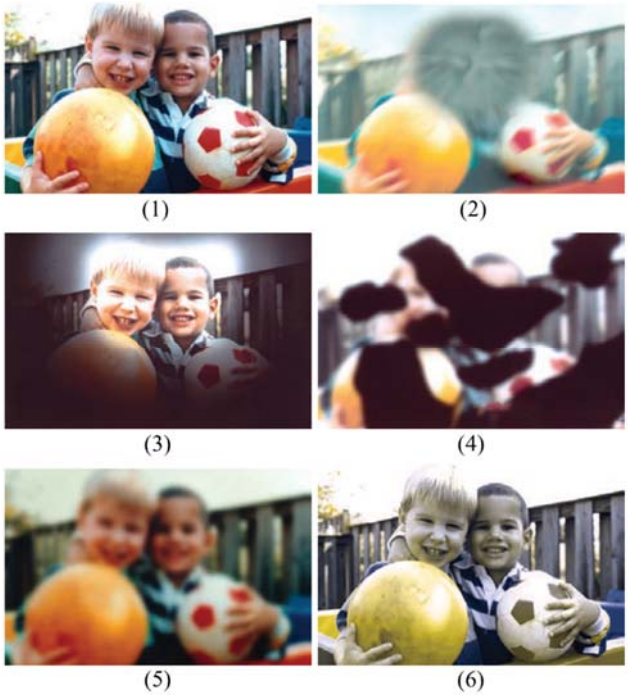


**Fig. 4** Visual impairment effects: (1) normal vision, (2) age-related macular degeneration, (3) glaucoma, (4) diabetic retinopathy, (5) cataract, (6) color vision deficiency

Diabetic retinopathy causes damage both to central and peripheral vision, as can be seen in Fig. 4 middle-right. As diabetes is a lifelong condition, treatment depends on the type of diabetic retinopathy and is aimed at slowing or stopping progression of the condition. Surgery often slows or stops the progression, but it's not a cure [6]. Visually impaired person with diabetic retinopathy induced damage could rely on some forms of assistive technology. However, VR headset based assistive technology would probably not be convenient as damaged areas are dispersed and of irregular shapes [5].

Cataract induces blur to both to central and peripheral vision, as can be seen in Fig. 4 bottom-left. It can be treated with a surgery [6]. Visually impaired person suffering from cataract could rely on some forms of assistive technology till the surgery. However, use of VR based assistive technology could not be justified as surgery to remove clouded lens and replace it with a clear, plastic intraocular lens would be more economical and would give much better results [5].

Color vision deficiency (CVD) is inability to distinguish certain shades of color, as can be seen in Fig. 4 bottom-right. CVD is inherited condition and cannot be cured [6]. Visually impaired person suffering from CVD would benefit from the use of assistive technology and specifically from VR headset based assistive technology

that could be used for a real time image correction aimed at transforming the full FoV image to a CVD friendly image.

Thus, virtual reality is a reasonable choice for assistive technology aimed at visually impaired persons affected with AMD, glaucoma and CVD. In case of AMD, VR based assistive technology is expected to have limited results due to the lack of a central vision. In case of glaucoma VR based assistive technology might have somewhat better results as central vision could be used to compensate peripheral vision damage. And finally, VR based assistive technology have a potential to give the best result if used by visually impaired persons affected by CVD [7]. CVD is caused by malfunction of photoreceptors in human eye retina and there are three classes of cones with photoreceptors susceptible to color: the first class is sensitive to long wavelength in the visible spectrum (L), the second class is sensitive to middle wavelength in the visible spectrum (M) and the third class of cones is sensitive to short wavelengths in the visible spectrum (S). Person with normal color vision has all three cone classes intact and is referred to as trichromat. Malfunction of any of the cone classes will result in CVD [5].

## 3. VIRTUAL REALITY TEST SETUP FOR CVD

Virtual headset uses PenTile AMOLED display with 2160×1200 resolution (1080×1200 per eye) and 456 ppi pixel density [8]. The display is refreshed at the 90 Hz rate and seen through hybrid Fresnel lenses enabling 110° field of view. User head motion is tracked using accelerometer, gyroscope and IR LED head tracking using external constellation camera enabling 6 degrees of freedom (6 DoF). Headset supports 3D audio and is connected to a personal computer with 4 meters long HDMI 1.3 and USB 3.0 cables [5] [7].

Stereo camera is based on two 1/3" backside illumination 4 million pixels image sensors with high low-light sensitivity [9]. The image sensors have synchronized rolling shutter, auto exposure, gain and white balance. The camera has *f*/2.0 aperture lenses that cover field of view 90° (H) x 60° (V) x 110° (D). The camera uses gyroscope and accelerometer to determine its position with +/- 1mm accuracy and orientation with +/-0.1° accuracy. Supported output video modes are: 2.2K mode with 4416x1242 output resolution at 15 frames per second, 1080p mode with 3840x1080 output resolution at 30 frames per second, 720p mode with 2560x720 output resolution at 60 frames per second, and WVGA mode with 1344x376 output resolution at 100 frames per second. In addition to the video, the camera outputs depth range for each pixel. Depth range is between 15 cm and 1200 cm [5] [7].

Image captured by the stereo camera is Red Green Blue (RGB) coded and this does not correspond to the human photoreceptor's sensitivity. That is why RGB color coding is not suitable for CVD image processing. Captured image must be converted to LMS color space to match L, M and S cones in the retina. Color space conversion is done by the following image processing transformation matrix [5] [7]:

$$\boldsymbol{M}_{RGB\rightarrow LMS} = \begin{bmatrix} 17.8824 & 43.5161 & 4.11935 \\ 3.45565 & 27.1554 & 3.86714 \\ 0.0299566 & 0.184309 & 1.46709 \end{bmatrix} \quad (1)$$

Transformation from LMS color space to RGB color space is done using inverse $\boldsymbol{M}_{RGB\rightarrow LMS}$ matrix [5] [7]:

$$\boldsymbol{M}_{LMS\rightarrow RGB} = (\boldsymbol{M}_{RGB\rightarrow LMS})^{-1} \quad (2)$$

Thus $\boldsymbol{M}_{LMS\rightarrow RGB}$ transformation matrix is as follows [7]:

$$\boldsymbol{M}_{LMS\rightarrow RGB} = \begin{bmatrix} 0.08094 & -0.13050 & 0.11672 \\ -0.01024 & 0.05401 & -0.11361 \\ -0.00036 & -0.00412 & 0.69351 \end{bmatrix} \quad (3)$$

Visually impaired person affected by CVD will see the image transformed into limited color space due to the lack of certain class of cones. Matrix that simulates CVD condition by transforming image into such limited color space is dependent on the class of cones missing [5] [7].

$$\boldsymbol{M}_{CVD} = \begin{cases} \boldsymbol{M}_{Prop} & if\ Protanopia \\ \boldsymbol{M}_{Deut} & if\ Deuteranopia \\ \boldsymbol{M}_{Trit} & if\ Tritanopia \end{cases} \quad (4)$$

Thus, visually impaired person affected by CVD will not see the original RGB colors, but rather colors given by the following transformation into a limited CVD color space [5] [7].

$$\begin{bmatrix} R_{CVD} \\ G_{CVD} \\ B_{CVD} \end{bmatrix} = \boldsymbol{M}_{LMS\rightarrow RGB}\ \boldsymbol{M}_{CVD}\ \boldsymbol{M}_{RGB\rightarrow LMS} \begin{bmatrix} R \\ G \\ B \end{bmatrix} \quad (5)$$

## 4. VISUAL IMPAIRMENT FRIENDLY RFID ROOM

Radio Frequency Identification (RFID) is a mature technology and frequently used in retail, storage, and logistics [5]. At its core, RFID system is composed of a reader and a tag, as can be seen in Fig. 5. The basic setup can be expanded to any combination of multiple readers and multiple tags to fit particular functional and spatial requirements [5]. Various object of interest are tagged to enable reader to localize them or determine their orientation

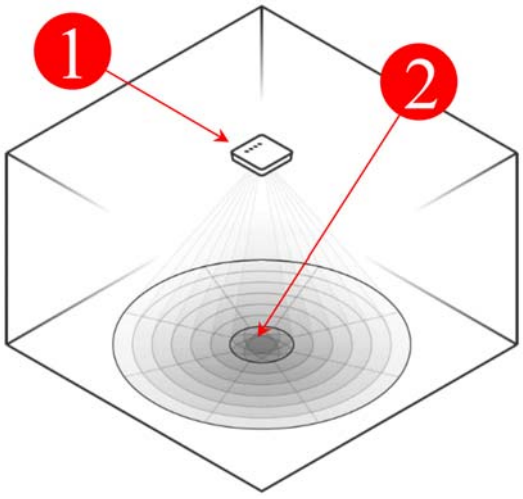


**Fig. 5** Visual Impairment Friendly RFID Room: (1) RFID reader at the ceiling, (2) Sector map of the covered region

or state, as can be seen in Fig. 6. The tag is composed of an antenna and an integrated circuit with preprogrammed unique identification code enabling identification to be performed over the wireless communication channel. Tag's integrated circuitry is by several orders of magnitude smaller than antenna, so the RFID tag size depends solely on the antenna size. Having a unique identification code enables tag to virtually represent unique surveyed object or a point of interest at the surveyed object. The major difference between RFID tags and other means of tagging, like bar codes, is the reading speed and reading penetration. RFID tags are superior if batch reading is required, particularly if large number of tags is dispersed over the region of interest with some of the tags out of the line of sight. From the standpoint of powering the tags, there is a major difference between active and passive tags. Active tag will require an external power source. Although the external source can be any power source with wired connection to the tag, the most common external power source would be an embedded battery. There are certain advantages to using the external power source, like the active tag being continuously operational and thus being able to process external signals, if required and supported by its additional integrated circuitry. However, passive tags have significant advantage over active tags when it comes to the system sustainability. Active tags require embedded battery to be replaced or recharged periodically. Even if active tags power consumption is highly optimized it will still pose a significant obstacle because the number of tags can be significant and it takes time to charge or replace the batteries - leaving the system in void or partially functional state. System based on passive tags will have no issues with sustainability as passive tags are rather affordable and do not have any time limit related to powering or any other longevity issue. The proposed setup is to enable visually impaired individuals to be as much independent as possible. Thus the use of active tags is not the best option as battery recharging and replacement would most likely require external assistance. On the other hand, the use of passive tags results in a sustainable system where external assistance might be required for the initial tagging only. We have evaluated passive tags [5] only as can be seen in Fig. 7.

1) DogBone RFID tag based on Monza R6 integrated circuit features two "dogbone" shaped antennas. Wet inlay


**Fig. 6** Various objects of interest tagged: (1) Chair with 3 tags attached, (2) desk with 2 tags attached, (3) book with a single tag, (4) desk drawer tagged with 2 tags attached

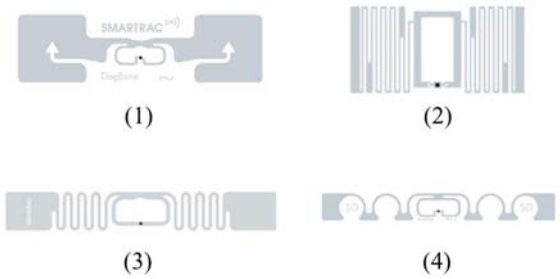


**Fig. 7** RFID tags used to evaluate the test setup: DogBone Monza 6 tag (1), BLING Monza 6 tag (2), Belt Monza 6 tag (3) and ShortDipole Monza 6 tag (4)

variant of the DogBone tag transmits in an omni-directional pattern eliminating blind spots. Thus the orientation of the tag and reader is less of a factor in the success of wireless communication. Monza R6 integrated circuit provides environmental auto-tune abilities that automatically adjust tag performance for best readability and higher sensitivity. Auto-tune feature can be programmatically turned on and off using low-level commands from the reader. Unlike other tags, the Dogbone integrated circuitry does not have user memory, which provides higher sensitivities and allows the potential for longer read ranges and faster read rates. It also has excellent performance on difficult-to-tag materials [5].

2) BLING RFID wet inlay tag is based on Monza R6 integrated circuit and designed for jewelry and cosmetics applications. It can be easily converted into small-sized hang-tags for jewelry labels, or attached to small cosmetic items. BLING comes in a tiny 22 mm form factor and is the smallest of all evaluated tags. Its intended use within the test setup is tagging small objects that can be found on the table, like pencils or books, or tagging larger objects that require multiple tags in order to determine their spatial orientation [5].

3) Belt RFID paper inlay tag is based on Monza R6 integrated circuit and designed for good tolerance and performance on difficult-to-tag or low-detuning materials such as cardboard and plastics and in other demanding environments. It is also a recommended tag for the phased array antenna xArray reader [5].

4) ShortDipole RFID paper tag is based on Monza R6 integrated circuit and offers excellent performance on lower detuning materials like cardboard, plastics, and corrugated boxes. ShortDipole tag comes in variety of delivery formats – dry, wet, and paper tag – making it suitable for all sorts of labels. In addition to Monza R6 integrated circuit auto-tune abilities that automatically adjust tag performance for best readability and higher sensitivity, ShortDipole tag circuitry supports Enduro technology for better consistency, and Integra technology for data integrity and reliability [5].

## 5. EXPERIMENTAL RESULTS

Major goal of the VR test setup is to enable assistive technology design and testing. Assistive device for CVD is supposed to transform the image as seen by the visually impaired person into an image that more closely resembles the original image, but is still bound to the limited CVD color space [10] [11] [12] [13] [14]. In order to do this,

image processing must focus on the visual information that visually impaired person misses due to its CVD condition. The missing information arise from the difference between the perceived image and original image [7]:

$$\begin{bmatrix} R_{\Delta CVD} \\ G_{\Delta CVD} \\ B_{\Delta CVD} \end{bmatrix} = \begin{bmatrix} R_{CVD} \\ G_{CVD} \\ B_{CVD} \end{bmatrix} - \begin{bmatrix} R \\ G \\ B \end{bmatrix} \tag{6}$$

Virtual reality based assistive device, at its core, performs image processing on the matrix (6) in order to render improved images – the ones that help CVD visually impaired person to better perceive the reality. Thus the VR test setup acts as a prototype assistive device [7].

### 5.1. VR Refresh Rate Evaluation

In order for the prototype to be functional it must not create noticeable delay between stereo camera captured reality images and presented transformed images. Virtual reality requires 90 Hz refresh rate and test setup must be able to achieve this rate with CVD image processing active and running. We have tested the VR setup using known transformation that has achieved positive results while evaluated on 24 visually impaired individuals with CVD condition [15]. The transformation uses following matrix for protanopia [7]:

$$\boldsymbol{A}_{Prop} = \begin{bmatrix} 0 & 0 & 0 \\ 0.5 & 1 & 0 \\ 0.5 & 0 & 1 \end{bmatrix} \tag{7}$$

Protanopia matrix (7) is used as $\boldsymbol{A}_{CVD}$ in (6) and added to the CVD image (5) that is to be improved [7]:

$$\begin{bmatrix} R' \\ G' \\ B' \end{bmatrix} = \begin{bmatrix} R \\ G \\ B \end{bmatrix} + \boldsymbol{A}_{CVD} \begin{bmatrix} R_{\Delta CVD} \\ G_{\Delta CVD} \\ B_{\Delta CVD} \end{bmatrix} \tag{8}$$

We have measured refresh rate that can be achieved while CVD image processing is running and results are shown in Fig. 8.

### 5.2. VR Time-Domain Color Mapping Evaluation

As the Ishihara test is usually used to disqualify those affected by CVD from certain occupations, we have adopted Ishihara test plates as a validation metric. Sample Ishihara plate can be seen in Fig. 9. Proposed time-domain color mapping is tested using virtual reality prototype implementing sinusoidal time-domain color mapping for protanopia as follows [7]:

$$\boldsymbol{A}_{Prop}(t) = \begin{bmatrix} 0 & 0 & 0 \\ \left(\frac{1+\sin(2\pi\omega t)}{2}\right) & 1 & 0 \\ \left(\frac{1-\sin(2\pi\omega t)}{2}\right) & 0 & 1 \end{bmatrix} \tag{9}$$

Parameter $\omega$ determines the number of color pulsations in a second and is set to 1 in the experiment. Without assistive image processing running, protanope under the test cannot read the number 8 on the Ishihara test plate as can be seen in Fig. 9. Once the assistive image processing based on (7) is started, protanope perceives the original image as seen in Fig. 10, plate (2). The number 8 on the plate becomes visible as greyish. When time-domain color mapping image processing based on (9) is started, the protanope under the test sees the number 8 on the Ishihara plate gradually changing its color from bluish through greyish to yellowish, and then back through greyish to bluish. The cycle repeats $\omega=1$ times in a second. All subjects have confirmed that number 8 becomes significantly more visible once the time-domain color mapping image processing is started. Majority agree that "yellowish glow", as can be seen in Fig. 10 plate (3), was particularly adding to a readability of the Ishihara test plate in the experiment [7].

### 5.3. RFID Tags Evaluation

X-Stage [16] shown in Fig. 11 is custom designed for tag spatial location evaluation and supports single axis

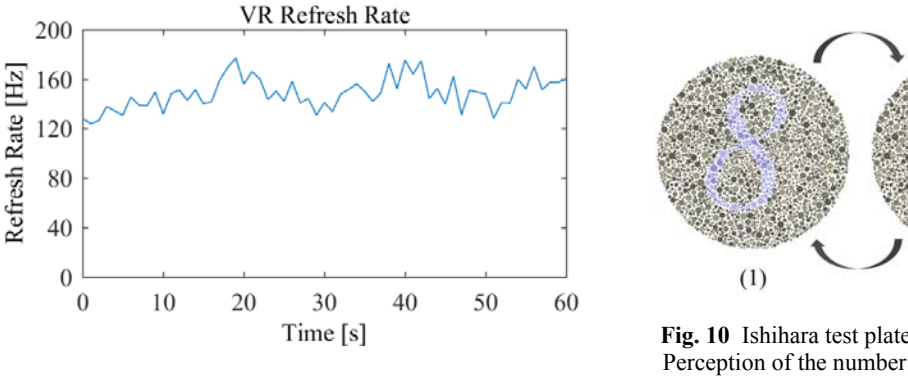


**Fig. 8** Virtual reality test setup CVD image processing refresh rate

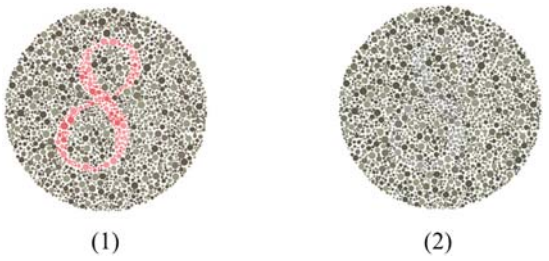


**Fig. 9** Ishihara test plate: (1) As seen by a person with normal vision, (2) As seen by a protanope

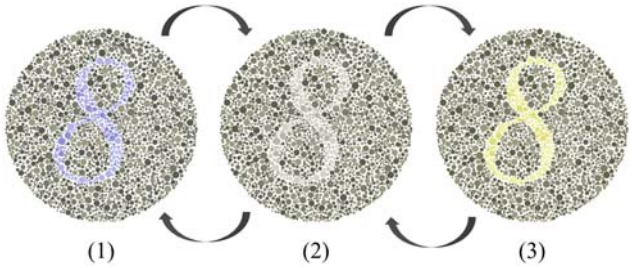


**Fig. 10** Ishihara test plate as seen by a protanope under the test. Perception of the number 8 changes from (1) bluish through (2) greyish to (3) yellowish; and then back through greyish to bluish. The cycle repeats ω times in a second

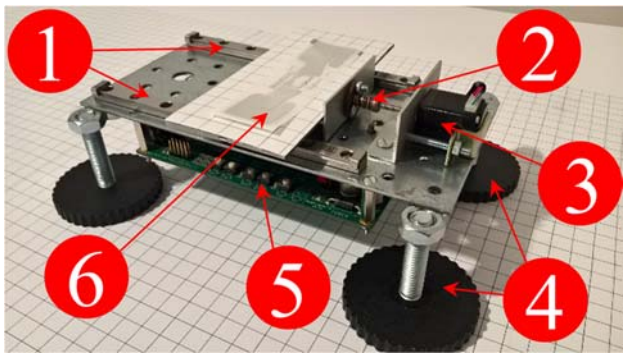


**Fig. 11** Custom designed X-Stage for fine tags spatial location evaluation. Ball slide guides (1), anti-backlash nuts (2), linear actuator (3), leveling and support structures (4), micro-stepper controller (5) and tag under the test (6)

target translation up to 100 mm in 10 micron repeatable steps. X-Stage main components are [5]:

1) Ball Slide Guides: enable smooth and repeatable linear translation of X-axis stage without yaw, pitch and roll [17]. Setup uses two 155 mm long preloaded ball slide guides mounted 70 mm apart to ensure high rigidity. Running parallelism for both vertical and horizontal ball slide guide planes is under 6 microns [5] [16].

2) Anti-Backlash Nuts: enable repeatable translation steps regardless of translation direction changes [18]. Travel direction changes induce small mechanical backlash that must be addressed. Anti-backlash nuts use preloaded spring to prevent backlash if axial load on the system is less than spring preload [5].

3) Linear Actuator: pushes and pulls X-axis stage by converting stepper rotation into anti-backlash nut linear travel. Setup uses hybrid linear actuator with external shaft precisely machined to convert 1.8º rotation steps into 10 micron linear steps. It can move 10 N loads at 1600 steps/second up to 25 N loads at 400 steps/second [5] [19].

4) Leveling and support Structures: enable accurate placing and fastening of components to the optical table or bench (XY plane) and adjusting their height (Z axis) manually. They also serve as vibration isolators [5] [19].

5) Micro-Stepper Controller: controls linear actuator and enables two additional stage axes to be controlled programmatically through software framework, if required. Controller uses two micro-switches as motion limiters and position references. Custom velocity profiles are used to ensure broad range of X-axis stage linear speeds that can be modified in real-time and still avoid stepper vibration and stall [5] [20] [21].

X-Stage is manually placed at desired distance from the reader. Tag under the test is placed on the X-Stage and moved along the preprogrammed path using micro-stepper motion controller connected to the personal computer. Personal computer is connected to the RFID reader over the network. It collects and stores RSSI and AoA readings into the database along with real-time tag position data coming from the micro-stepper motion controller [5]. Stored data can be later processed in order to test and improve accuracy of RFID spatial position estimator algorithms. The major factor to the spatial position estimation is number of tag reads. Spatial position estimation will be more accurate with higher number of tag reads [5]. All evaluated tag types

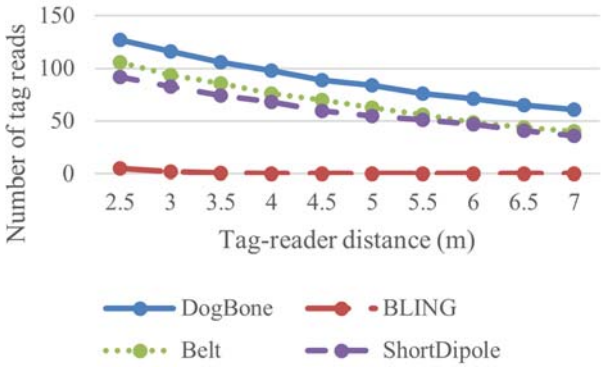


**Fig. 12** Number of tag reads vs. tag-reader distance for all evaluated tag types

have been tested for number of reads in a limited amount of time [5] and results are shown in Fig. 12.

### 5.4. RFID Spatial Localization Evaluation

RFID reader uses phased array antenna radio frequency beam that tends to be narrow but is still significantly wider than focused beam of light. Phased array antenna beam is actually composed of several lobes: main lobe, back lobe and side lobes. The major factor determining reader's phased array antenna beam diameter is the main lobe. Spatial information accuracy based on the AoA depends on the beam diameter and it gets worse as the main lobe gets wider. In reality, two arrival angles, $\theta_T$ and $\Phi_T$, point to the center of the area where tag might be located. This area is sometimes referred to as sector and determined by the intersection of the main lobe with the surveillance plane. Surveillance plane is thus divided into sectors and AoA can provide information about the sector in which the tag is located. Although the RFID reader's spatial coverage is often represented by the map divided into neighboring sectors with clear borders, in reality sectors overlap. Thus, RFID reader will almost always detect any single tag to be located in multiple sectors at any point in time. To deal with this issue, various algorithms based on multiple readings of each and every tag can be adopted. PATL algorithm calculates the centroid of the polygon consisting of the line segments among the centers of sectors where the tag is read. If the total number of sectors where the tag is read is $M$, and if center points of sectors are $P_1, P_2 \ldots, P_M$, then tag location is [22]:

$$\begin{bmatrix} x \\ y \end{bmatrix} = \begin{bmatrix} \sum_{i=1}^{M} \frac{1}{M} \cdot x_{P_i} \\ \sum_{i=1}^{M} \frac{1}{M} \cdot y_{P_i} \end{bmatrix} \tag{10}$$

If average sector size is larger than required spatial location precision then additional steps may be introduced to differentiate between tags based on their relative distance to the center of the sector. If a tag is located in the center of the sector then it will receive maximum signal strength from the front lobe of the beam. Consequently, the tag will

be read more frequently than a tag located further away from the center of the sector. Thus, the ratio of tag reads $n_i$ in any particular sector and the total number of reads can be used as a normalized weighting factor $w_i$ for that sector [22]:

$$w_i = \frac{n_i}{\sum_{j=1}^{M} n_j} \tag{11}$$

Weighted PATL spatial location of the tag is [22]:

$$\begin{bmatrix} x \\ y \end{bmatrix} = \begin{bmatrix} \sum_{i=1}^{M} w_i \cdot x_{P_i} \\ \sum_{i=1}^{M} w_i \cdot y_{P_i} \end{bmatrix} \tag{12}$$

PATL results can additionally be averaged with center points of sectors based on the RSSI, as described in EPATL localization algorithm [22]. However, we have noticed that localization accuracy tends to fall significantly as we move tags away from the covered region center. Thus we propose use of multiple readers with overlapping regions in order to improve and equalize accuracy. Resulting spatial location is calculated as centroid of the polygon consisting of $K$ neighboring readers' PATL results [22].

$$\begin{bmatrix} x \\ y \end{bmatrix} = \begin{bmatrix} \sum_{i=1}^{K} \frac{1}{K} \cdot x_{PATL} \\ \sum_{i=1}^{M} \frac{1}{K} \cdot y_{PATL} \end{bmatrix} \tag{13}$$

We have tested proposed localization algorithm using two xArray readers mounted 5 meters away from each other [22] and results can be seen in Fig. 13.

## 6. CONCLUSIONS

We have proposed a test setup for visually impaired assistive technology. In order to understand the effects of various visual impairments we have compared the benefits of existing treatments to the use of assistive technology. We have specifically estimated if virtual reality (VR) based assistive technology would be a reasonable choice for certain visual impairments. We affirm that virtual reality is a reasonable choice for assistive technology aimed at visually impaired persons affected with AMD, glaucoma and CVD. In case of AMD, VR based assistive technology is expected to have limited results due to the lack of a central vision. In case of glaucoma VR based assistive technology might have somewhat better results as central vision could be used to compensate peripheral vision damage. And finally, we affirm that VR based assistive technology have a potential to give the best results if used by visually impaired persons affected by CVD. We have tested proposed setup as a prototype assistive device for protanopia using known color transformation and have achieved real-time performance. We have proposed a time-domain color mapping to improve Ishihara test scores. Experimental results confirmed that Ishihara plates become significantly more readable once virtual reality prototype starts the time-domain color mapping image processing based on a sinusoidal envelope

Visual Impairment Friendly Room based on RFID is proposed to enable object localization and its use by visually impaired persons. Various tags types have been evaluated. The DogBone tag proved to have the highest number of tag reads across a range of reader-tag distances and is preferred tag for spatial position estimation. Algorithm enhancement for object localization based on use of multiple readers with overlapping regions is proposed in order to improve and equalize accuracy. Experimental results show that proposed algorithm has better overall accuracy as it does not tend to significantly change as tags move away from the covered region center.

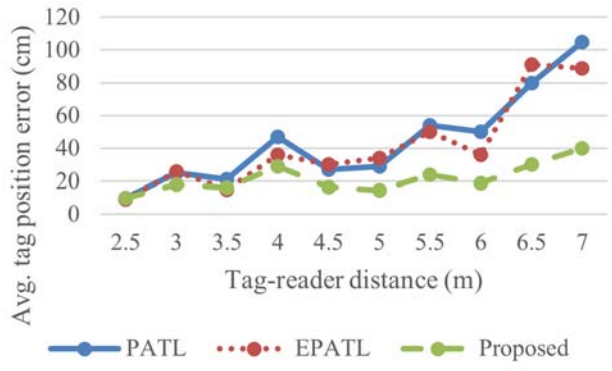


**Fig. 13** Average estimated tag position error vs. tag-reader distance for PATL, EPATL and proposed algorithm

## ACKNOWLEDGMENTS

We express our appreciation to the local partners for allowing us to use their NVIDIA GPUs and image capturing equipment for this work.

This work was supported by the Federal Ministry of Education and Science.

## REFERENCES

[1] National Eye Institute, http://www.nei.nih.gov. Accessed 2020-02-14.

[2] Statistics Botswana, Eye Disease Statistics 2014, http:// http://www.statsbots.org.bw. Accessed 2020-02-14.

[3] European Society of Retina Specialists, http://www.euretina.org. Accessed 2020-02-14.

[4] World Blind Union (WBU), http://www.worldblindunion.org. Accessed 2020-02-14.

[5] BESIC, I. – AVDAGIC, Z. – HODZIC, K.: "Virtual Reality Test Setup for Visual Impairment Studies," *2019 IEEE 15th International Scientific Conference on Informatics*, Poprad, 2019.

[6] Mayo Clinic, Diseases & Conditions, https://www.mayoclinic.org/. Accessed 2020-02-14.

[7] BESIC, I. – OMANOVIC, S. – BOSKOVIC, D.: "Time-Domain Color Mapping for Color Vision Deficiency Assistive Technology," *2019 2nd International Conference on Signal Processing and Information Security (ICSPIS)*, DUBAI, United Arab Emirates, 2019.

[8] Oculus Rift, https://www.oculus.com. Accessed 2020-02-14.

[9] StereoLabs ZED Mini, https://www.stereolabs.com, Accessed 2020-02-14.

[10] PRAMOUN, T. – THONGKOR, K. – AMORNRAKSA, T.: "Image watermarking against color blind image correction," *2017 10th International Conference on Ubi-media Computing and Workshops (Ubi-Media)*, Pattaya, 2017, pp. 1-6.

[11] KVITLE, A. K. – ODDLØKKEN, H. – GREEN, P – NUSSBAUM, P.: "Methods for psychophysical assessment of colour difference by observers with a colour vision deficiency," *2018 Colour and Visual Computing Symposium (CVCS)*, Gjøvik, 2018, pp. 1-6.

[12] YOU, J. I. – PARK, K.: "Image Processing With Color Compensation Using LCD Display for Color Vision Deficiency," in *Journal of Display Technology*, vol. 12, no. 6, pp. 562-566, June 2016.

[13] ZHANG, L. *et al*.: "Improved colour-to-grey method using image segmentation and colour difference model for colour vision deficiency," in *IET Image Processing*, vol. 12, no. 3, pp. 314-319, 3 2018.

[14] CHEN, Y. – CHAO-YAN ZHOU – LONG-YUN LI, "Perceiving stroke information from color-blindness images," *2016 IEEE International Conference on Systems, Man, and Cybernetics (SMC)*, Budapest, 2016, pp. 000070-000073.

[15] MELILLO, P. *et al*.: "Wearable Improved Vision System for Color Vision Deficiency Correction," in *IEEE Journal of Translational Engineering in Health and Medicine*, vol. 5, pp. 1-7, 2017, Art no. 3800107.

[16] BESIC, I. – AVDAGIC, Z.: "Automated test environment for image processing in laser triangulation 3D scanning," *2016 International Symposium ELMAR*, Zadar, 2016, pp. 161-164.

[17] HSU, W. C. – CHANG, C. S.: "Linear ball guide assembly," United States Patent 5,429,439, Jul. 4, 1995.

[18] ERIKSON, K. W.: "Adjustable preload anti-backlash nut ," United States Patent 5,913,940, Jun. 22, 1999.

[19] BESIC, I. – AVDAGIC, Z.: "Laser stripe sub-pixel peak detection in real-time 3D scanning using power modulation," *IECON 2016 - 42nd Annual Conference of the IEEE Industrial Electronics Society*, Florence, 2016, pp. 951-956.

[20] DWERSTEG, B. – LARSSON, L.: "Method and circuit arrangement for sensorless engine load detection and for controlling the motor current in accordance with the load value in stepper motors ," United States Patent Application Publication US 2012/0153886 A1, Jun. 21, 2012.

[21] BESIC, I. – AVDAGIC, Z.: "Laser stripe model for sub-pixel peak detection in real-time 3D scanning," *2016 IEEE International Conference on Systems, Man, and Cybernetics (SMC)*, Budapest, 2016, pp. 004332-004337.

[22] BESIC, I. – AVDAGIC – HODZIC, Z. K.: "RFID Based Indoors Test Setup for Visually Impaired," *2019 11th International Conference on Electrical and Electronics Engineering (ELECO)*, Bursa, Turkey, 2019, pp. 465-469.

Received February 26, 2020, accepted May 26, 2021

## BIOGRAPHIES

**Ingmar Bešić** graduated with distinction in 2000 at the Department of Computer Science and Informatics of Faculty of Electrical Engineering of the University of Sarajevo. He received MSc degree in Software Engineering in 2004 from the Keble College at the University of Oxford. In 2016 he received PhD degree from the Faculty of Electrical Engineering of the University of Sarajevo. His research interests are computer vision, real-time systems, software engineering, artificial intelligence, bioinformatics, computer assisted design and manufacturing and 3D scanning. He is currently assistant professor at the Faculty of Electrical Engineering, University of Sarajevo.

**Zikrija Avdagić** is a professor at the University of Sarajevo-Faculty of Electrical Engineering Sarajevo-Department for Computing and Informatics, covering field of Artificial Intelligence and Bioinformatics. He received his BSc, MSc. and DSc. degrees from the University of Sarajevo. In 2001 he was awarded the Fulbright Award for research related to intelligent control systems. His latest research is related to: Impact of Nuclear Domains On Gene Expression and Plant Traits, Statistical and machine learning techniques in human microbiome studies, and Real-time image processing for 3D computer vision for the visually impaired, in which he implements the fusion of artificial intelligence methods into microarray gene bioinformatics, nucleus bioprocessing and the prediction of cancer treatment based on human microbiome control.

**Kerim Hodžić** Kerim Hodžić was born in 1992 in Sarajevo, Bosnia and Herzegovina. He received his BoE degree in 2014 and MoE degree in 2014 from the Department for Computer Science and Informatics, Faculty of Electrical Engineering, University of Sarajevo where he works as a teaching assistant. He is currently a PhD student and has published 12 scientific papers in areas of his research interest: artificial intelligence, logistics, supply management, demand forecasting, order picking, GPS tracking, optimisation algorithms, virtual reality and CAD.